Geophysical Characterization of Carbonate Reservoirs Using Advanced Interpretation Techniques: Applications to Abenaki Formation, Penobscot Block, Nova Scotia*

D. Coronel[1], E. Villamizar[1], E. Illidge[1], and S. Khurama[1]

Search and Discovery Article #42083 (2017)**
Posted August 21, 2017

*Adapted from extended abstract prepared for poster presentation given at AAPG Annual Convention and Exhibition, April 2-5, 2017, Houston, Texas

[1]Universidad Industrial de Santander, Bucaramanga, Santander, Colombia (daniel22-4@hotmail.com)

Abstract

Due to the finite nature of hydrocarbons, it is more complicated and expensive to find them. Because of this, unconventional reservoirs have become an important source of hydrocarbon production, such as Shale Gas, Oil Shale and Carbonates. In this context, carbonate reservoirs could represent new opportunities; however, there is still lack of their understanding. Therefore, it is vital to integrate and apply new technologies and knowledge to reduce the risk during the exploration phase. Now, by integrating rock physics, seismic data and regional geology as an industry, geoscientists aim to characterize reservoirs in a more realistic and integrated way (Avseth et al., 2005). The AVO technique was developed to analyze pre-stack seismic data to characterize reservoirs and evaluate anomalies related to hydrocarbon accumulations (Rutherford and Williams, 1989). It is based on how the seismic amplitude varies with offset, which effect is linked to the rock mechanic-elastic properties. These changes in the reflectivity are the result of the contrasts between the P-wave and S-wave velocities and the density. Through its application, it is possible to generate models of properties, such as Poisson's moduli, Bulk moduli, and so on, which also control the seismic response. Using the seismic inversion, it is possible to turn the seismic amplitude into rock properties with the goal of obtaining a 3D model of the subsurface to be calibrated with the seismic and well data available. This will allow reduction of the uncertainty in the areas where there is no well data (Gharaee, 2013). The main objective of this study is to characterize carbonate reservoirs within the Abenaki Formation by integrating rock physics and seismic data.

Introduction

The variation of amplitude with offset is due to the so-called energy partitioning. In this context, when a wave front reaches a boundary part of the energy is reflected and part of it is transmitted. Now, for the case when the angle of incidence is not zero, the energy of the incident P wave is further divided into reflected and transmitted P & S components. The amplitude of the reflected and transmitted energy depends on the contrast of the physical properties across the boundary (Burianyk, 2000). On the other hand, extended exploratory projects have remarkably improved the understanding of offshore basins, such as Southern Danish North Sea (Back et. al. 2011), which have been explored over the past few decades in order to find the most profitable plays. In this context, the AVO technique provides vital information when defining the areas and intervals where there might be hydrocarbon accumulation, especially gas. Now, the application of AVO in carbonate reservoirs is not as straightforward as it is in sandstone reservoirs, since carbonates reservoirs have higher acoustic impedance values than those of sandstone reservoirs. Mainly for this reason, the changes of amplitude with increasing offset are not that clear and depend on the physical properties of the carbonate rock, especially on porosity and fluid saturation.

The goal of this study is to show how the results and interpretation of the integration of different advanced techniques of geological and geophysical data led to the generation of a quantitative geophysical model that accounts for the characterization of the carbonates found in the Penobscot Block Limestone complex of the Abenaki Formation.

Data and Methodology

For this analysis, a PSTM volume was used as well as the CMP gathers to get the PSTM model. The well dataset consists of two wells L-30 and B-41, but only the first one was used because it reaches the target formation.

The 3D-seismic data was acquired in the Nova Scotia offshore. It has a 12.5x25 [m] bin size, a sample interval of 4 [ms], an inline and crossline length of 12004 [m] and 7497 [m], respectively, and a time range of 0 – 6000 [ms] (Figure 1). The CMP gathers have an offset range of 175 – 3175 [m]. The well data consists of core descriptions and the logs available for this study are given in Table 1. Figure 2 shows the workflow used to generate the final model. In the following sections, all the steps and results are briefly explained. It is important to mention that the study area might not have relevance economically. However, the analysis made here contributes to the understanding of the carbonate rock physics and seismic behavior which represent a step forward in building a methodology for reservoir characterization that might be applied in this sort of play.

Regional Geological Setting

The Scotian Shelf is located in the eastern North American margin that was developed over the fractured continental edge of the North American plate (Figure 3) (Quayyum et al., 2014). During the Late Triassic to Early Jurassic rifted highs, lows and depocenters were developed (Welsink et al., 1989). The formation of a passive margin resulted in a postrift stratigraphic succession. The marine environments allowed the development of large-scale carbonate bank, known as the Abenaki Formation, during this period of development of the Scotian Shelf (Eliuk, 1978; Jansa, 1981; Weissenberger et al., 2006). The Abenaki Formation corresponds to shallow-marine deposits and consists mostly of limestones, dolomites, reefs, and mudstones. It is divided into four members, which are the Scatarie, Misaine, Baccaro and Artimon Members (Figure 4) (Eliuk, 1989; Ellis, Crevello and Eliuk, 1985; Eliuk and Levesque, 1998, Wierzbicki, Harland and Eliuk, 2002). The Baccaro Member is the best developed carbonate unit, and its lithology is mainly limestone with minor shale and sand intervals representing the reworked remnants of lowstand events (Kidston et al, 2005).

Well Log Interpretation

The next step in the workflow is the well log analysis. Core descriptions were tied to the well log data in building the rock-type model. This information was integrated with the implementation of methodologies, such as Vshale interpretation and crossplot classification (Figure 5) to obtain a 1D facies model calibrated with core descriptions. By using crossplots the interpreter can associate up to three different rock properties per crossplot, thus finding clusters of points in a crossplot that share similar ranges of the rock properties used as input data. Therefore, the clusters defined during the application of crossplots interpretation will represent a specific rock type with a given range of porosity, shale fraction, resistivity, density, P-wave and S-wave velocity, photoelectric factor, etc. By performing rock type classification using this methodology, the interpreter will be able to differentiate an low-porosity limestone from a high-porosity limestone, which is crucial when performing reservoir characterization in carbonate plays. Additionally, the classification of different types of claystone may also be performed by applying crossplot interpretation. However, it is highly recommended to use stratigraphic columns generated from the description of core and cuttings samples as input data to calibrate all of the interpretations of rock types made from crossplots or any other methodology. Figure 6 shows the resulting rock type profile for the correlation well calibrated with the rock types found in the core description. As mentioned in the description of the dataset, the correlation wells have no S-wave information; therefore it was necessary to implement one of the correlations found in the literature for this purpose. Once the rock type model is defined, it is possible to generate an S-wave velocity model using the Greenber-Castagna relationships (Figure 7). It is important to mention that for each rock type a different Vs trend was assigned; that would guarantee the shear impedance contrast between different rock types. This model was used along with the P-wave velocity and density logs to estimate the elastic properties. Crossploting these properties allowed the feasibility analysis (Figure 8).

Gassmann Fluid Substitution

The Gassmann fluid substitution theory is a useful tool when studying seismic attributes, amplitude variation with offset (AVO) or 4D response. It consists of modeling the effects of mineral, fluid and porosity on the seismic velocities based on empirical relationships and theoretical formulations (Smith et al., 2003; Avseth et al., 2005).

Before doing the fluid substitution, a complete petrophysical model was generated for the correlation well (Figure 9). Now, two main conclusions were made from the petrophysical model: the first one and perhaps the most important, the limestones in Abenaki Formation have a 100% water saturation; the second one, the total porosity for most of the limestone is about 2%. In this context, based on the information of water saturation that was obtained, a Gassmann fluid substitution was performed for different scenarios of water saturation and porosity in the carbonates of Abenaki Formation, with the goal of understanding how these factors affect elastic properties of carbonates, such as acoustic impedance and VpVs ratio. All the different scenarios of water saturation and porosity were modeled before a rock physics template for carbonates was prepared where these variations may be interpreted (Figure 10). The compressibility of the dry rock can be expressed by the following expression (equation 1):

$$1/KDry = 1/K_{Mineral} + 1/K_{\emptyset} \qquad (1)$$

Where K_{Dry} is the dry rock bulk modulus, $K_{Mineral}$ is the mineral bulk modulus and $K_{\emptyset}$ is the pore space stiffness.

Analogously, the next approximation expresses the compressibility for a saturated rock (K_{Sat}) (equation 2):

$$1/KSat \approx 1/K_{Mineral} + \emptyset/(K_{\emptyset}+K_{Fluid}) \qquad (2)$$

where K_{Fluid} is the pore-fluid bulk modulus. Figure 11 shows a particular example of the fluid substitution performed at 20% porosity and 40% of water saturation. It can be clearly seen how the elastic properties change from the original condition (2% porosity and 100% water saturation obtained from the petrophysical modeling made for well L-30) to the modeled condition.

AVO Modeling

Using the fluid substitution results, synthetic gathers were obtained for several scenarios using the Zoeppritz equation where total porosity and water saturation were replaced to analyze how the seismic gathers would appear if the limestone interval was saturated with gas and had higher porosity. Figure 12 shows an example of the synthetic gather modeling where the porosity and water saturation were modified to 20% and 0%, respectively, compared with the original seismic gather at the well position. As a conclusion of the AVO modeling, a plot was made where all the synthetic gathers pickings were compared with the original seismic gather (Figure 13). In his plot one can clearly see that the Abenaki Limestone is 100% saturated with water (concluded from the behavior of the picking made on the original seismic).

Seismic Image Conditioning and Input Data for Horizons and Fault Interpretation

After performing the seismic-well tie process, the interpretation of the 3D seismic data began by conditioning the seismic image. This process included interpretation of relative dip reflector and the enhancement of both the continuityof reflectors and faults. Based on the reflector dip attribute called Dip Steering (which was calculated using Opendtect) a set of about 200 horizons were tracked; they follow nicely the reflectors and therefore represent time lines that may be used in the following steps. Figure 1 illustrates the conditioned seismic image and the 3D horizon corresponding to the top of Abenaki.

AVO Analysis

Once the seismic gathers were conditioned (Figure 14) and the velocity model was calibrated using well logs, a set of AVO attributes was generated to analyze the possible anomalies present in the Abenaki limestones. Figure 15 shows the gradient-intercept crossplot made for the Abenaki limestones. Based on the analysis of AVO attributes and the expected behavior concluded from the synthetic analysis, a gradient-intercept anomaly was interpreted at a high structure on the Abenaki limestones (Figure 16). As it can be seen in Figure 17, the structure drilled at the location of well L-30 is dry; both the AVO anomaly observed in the Scaled Poisson's Ratio Change section and the petrophysical model support it. On the other hand, an interesting interval was found in the Abenaki Formation (Figure 16) that might have gas saturation and/or high porosity according to the anomalies identified in the AVO attributes. The difference between these carbonates is also shown in the Gradient-intercept attribute (Figure 18).

Conclusions

Rock type classification by crossplot interpretation allows the integration of different rock properties and their tie to the core description efficiently; this resulted in the identification of different lithotypes.

A better estimation of the S-wave velocity is achieved by including the rock classification since it allows the interpreter to use the adequate trend for a given rock type.

A rock physics template was obtained from modeling of different scenarios in the carbonate properties calibrated for the study area.

The dry- and low-porosity carbonates show positive gradient and intercept values while an anomalous zone is characterized by a positive gradient and a negative intercept; this zone shows a similar Poisson's ratio change in response of the underlying sandstones.

Selected References

Avseth, P., T. Mukerji, and G. Mavko, 2005, Quantitative seismic interpretation: Applying rock physics to reduce interpretation risk: Cambridge University Press.

Back, S., Gent, H., Reuning, L., Grötsch, J., Nierderau, and J., Kukla, P. 2011. 3D Seismic Geomorphology and Sedimentology of the Chalk Group, Southern Danish North Sea: Journal of the Geological Society, London, v. 168, p. 393–405.

Burianyk, M., and S. Pickford, 2000. Amplitude-Vs-Offset and Seismic Rock Property Analysis: A Primer: CSEG Recorder. Feature Article.

Campbell, T., F.W. Richards, L. Silva, G. Wach, and L.S. Eliuk, 2015, Interpretation of the Penobscot 3D seismic volume using constrained sparse spike inversion, Sable sub-Basin, offshore Nova Scotia: Marine and Petroleum Geology, v. 68, part A, December, Pages 73-93.

Ellis, P.M., P.D. Crevello, and L.S. Eliuk, 1985, Upper Jurassic and Lower Cretaceous deep-water buildups, Abenaki Formation, Nova Scotian Shelf, *in* P.D. Crevello and P.M. Harris, editors, Deep-water Carbonates: Society of Economic Paleontologists and Mineralogists, Special Publication 25 (Core Workshop no. 6), p.212-248.

Eliuk, L.S. 1978, The Abenaki Formation, Nova Scotia Shelf, Canada: A depositional and diagenetic model for a Mesozoic carbonate platform: Bulletin of Canadian Petroleum Geology, v. 26, p. 424–514.

Eliuk, L.S. and G. Wach, 2009, Carbonate and siliciclastic sequence stratigraphy — Examples from the Late Jurassic Abenaki Limestone and West Venture deltaic beds, offshore Nova Scotia, Canada (abstract): Presented at CSPG/CSEG/CWLSGeoConvention. Website accessed May 21, 2017, http://www.searchanddiscovery.com/pdfz/abstracts/pdf/2013/90171cspg/abstracts/ndx_eliu.pdf.html.

Greenberg, M.L., and J.P. Castagna, 1992, Shear-wave velocity estimation in porous rocks: Theoretical formulation, preliminary verification and applications: Geophysical Prospecting, v. 40, p. 195–209.

Jansa, L. F., 1981, Mesozoic carbonate platforms and banks off the eastern North American margin: Marine Geology, v. 44, p. 97–117.

Kidston, A.G., D.E. Brown, B.M. Smith, and B. Altheim, 2005, The Upper Jurassic Abenaki Formation Offshore Nova Scotia: A Seismic and Geologic Perspective: Canada- Nova Scotia Offshore Petroleum Board.

Qayyum, F., O. Catuneanu, and P.F.M. de Groot, 2013, Developments and future trends in Wheeler diagrams: 75th Annual International Conference and Exhibition, EAGE, Extended Abstracts, Tu0906.

Smith, T.M., C.H. Sondergeld, and C.S. Rai, 2003, Gassmann fluid substitutions: A tutorial: Geophysics, v. 68, p. 430-440.

Weissenberger, J.A.W., R.A. Wierzbicki, and N.J. Harland, 2006, Carbonate sequence stratigraphy and petroleum geology of the Jurassic Deep Panuke Field, offshore Nova Scotia, Canada, *in* P.M. Harris, and L.J. Weber, editors, Giant hydrocarbon reservoirs of the world: From Rocks to Reservoir Characterization and Modeling: AAPG, Memoir/SEPM Special Publication, v. 88, p. 395–431.

Wierzbicki, R.A., N.J. Harland, and L.S. Eliuk, 2002, Deep Panuke and Demascota core from the Jurassic Abenaki Formation, Nova Scotia – Facies Model, Deep Panuke, Abenaki Formation: Canadian Society of Petroleum Geologist Diamond Jubilee Convention, CD-ROM of Abstracts, Technical Talks, Posters & Core Displays, Paper no.12345678, 31p.

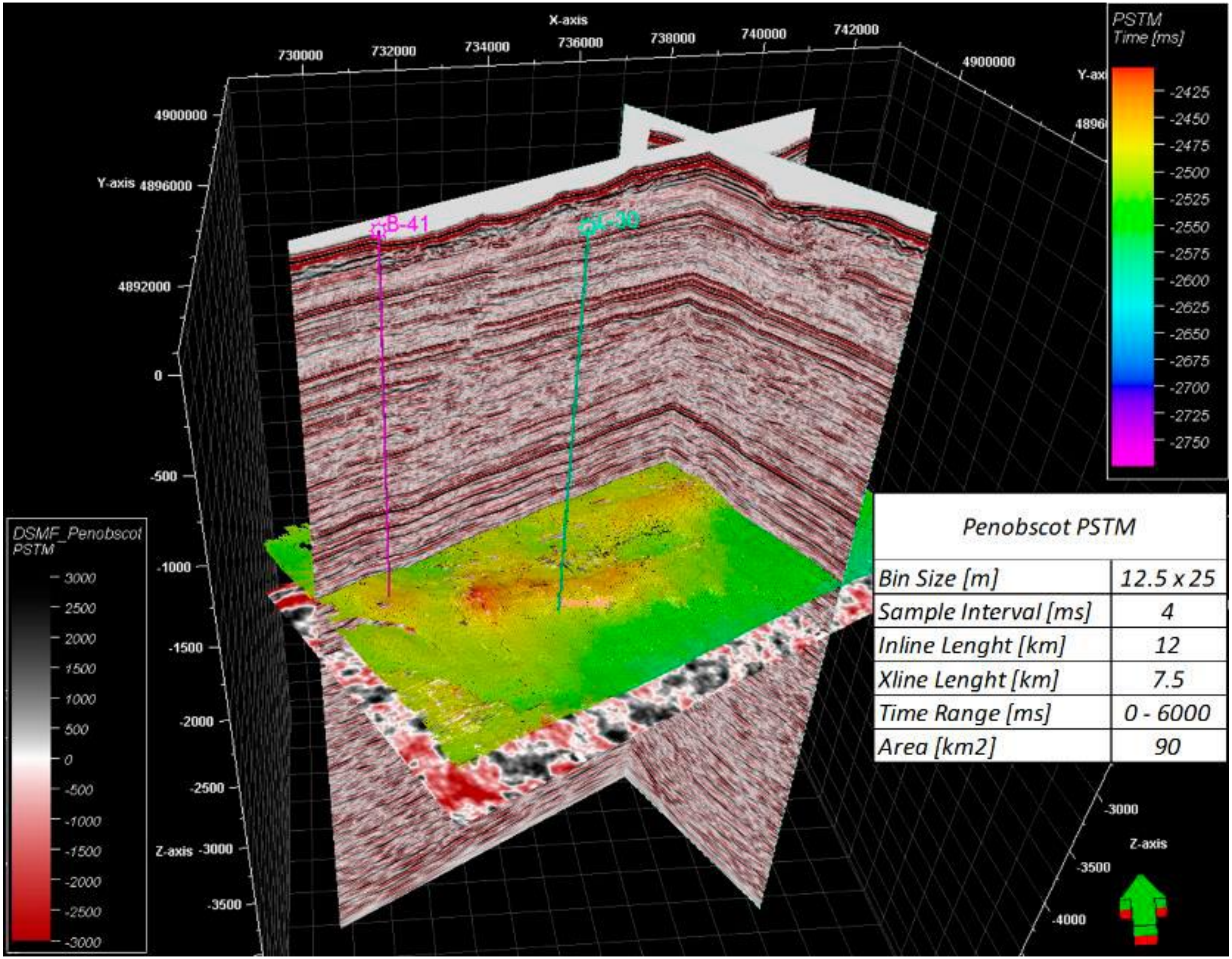

Figure 1. 3D seismic information and wells available in the study area.

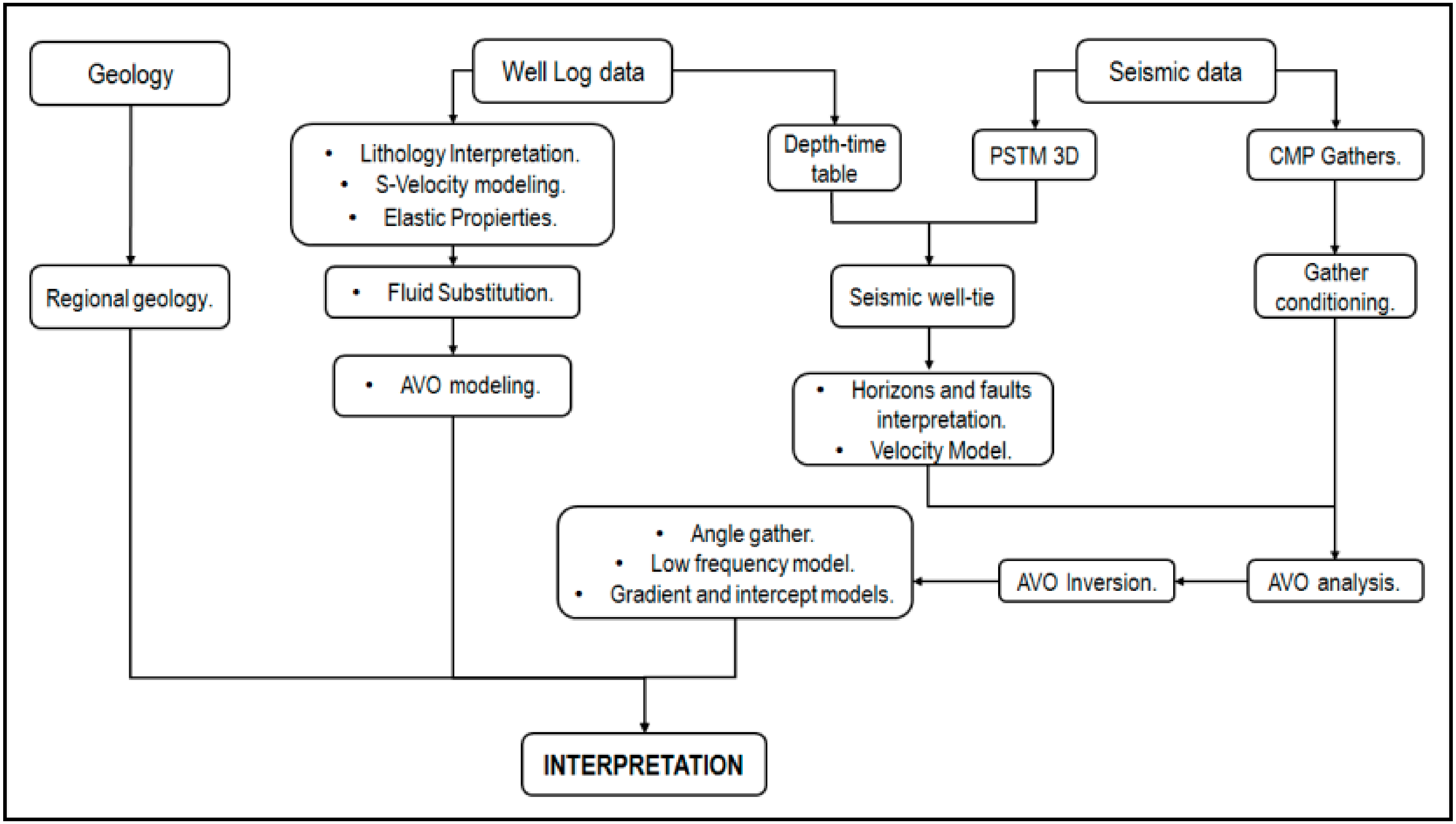

Figure 2. Workflow applied to transform petrophysical and geophysical information into a 3D geological model.

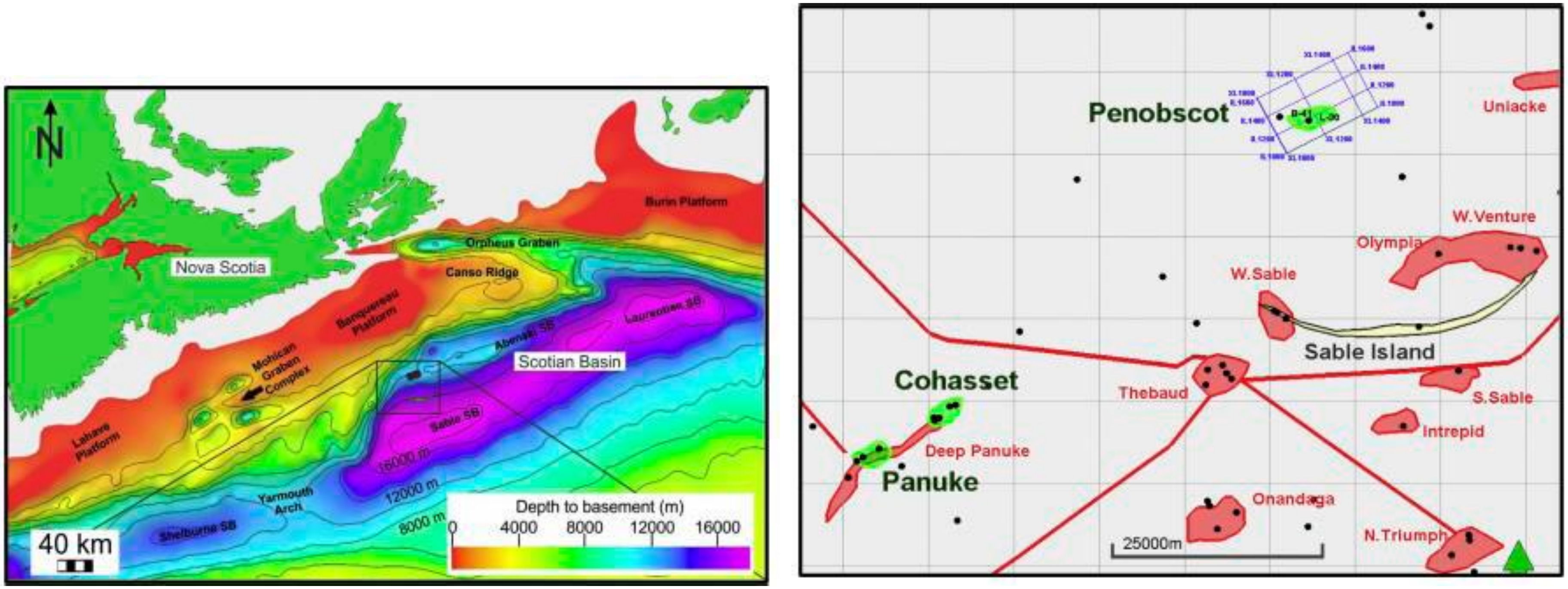

Figure 3. Scotian shelf sub-basins and location of the Penobscot 3D, wells and nearby fields, and pipelines. From Campbell et al., 2015.

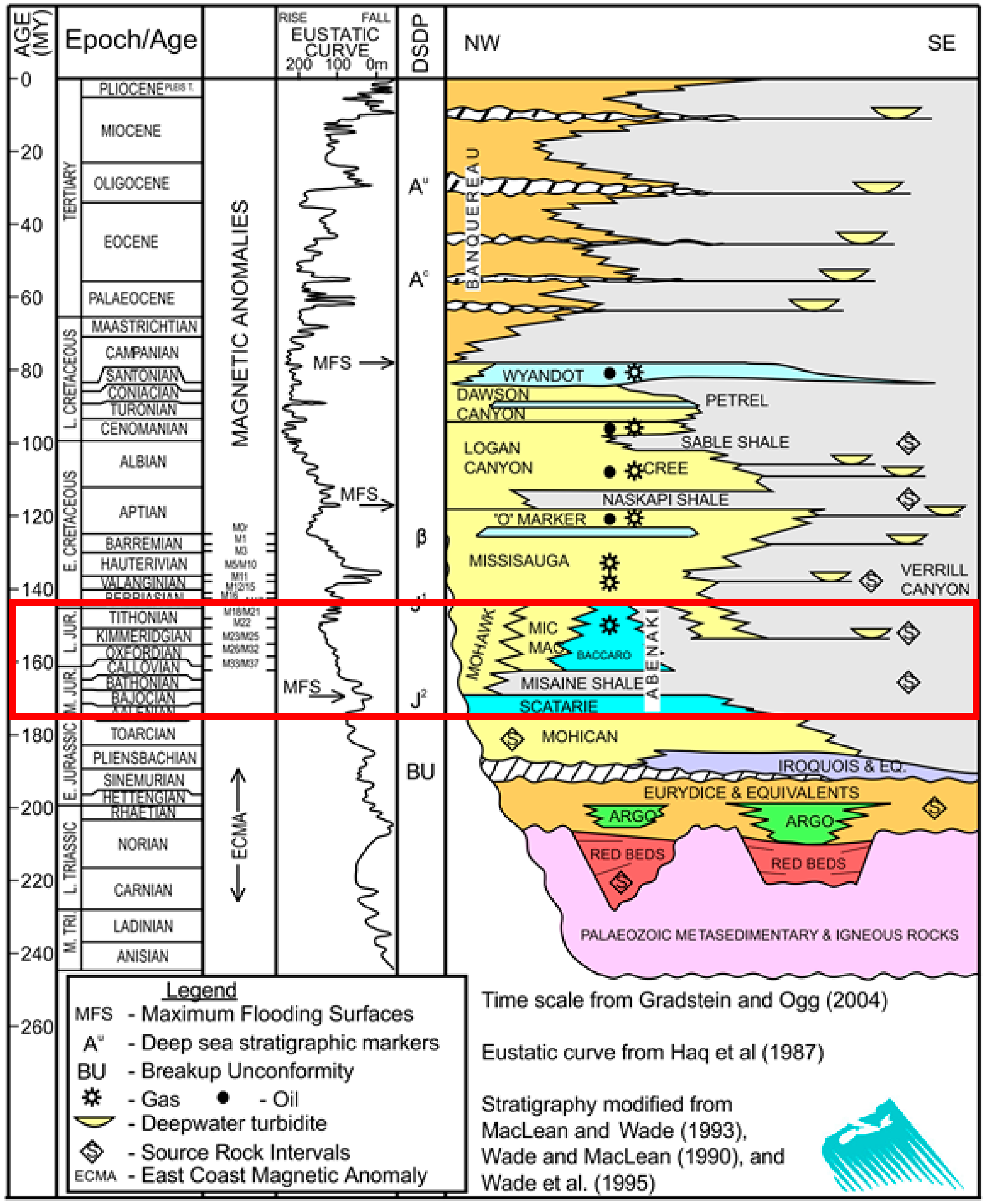

Figure 4. Generalized stratigraphic column of Nova Scotia basin. Modified from Kidston et al., 2005.

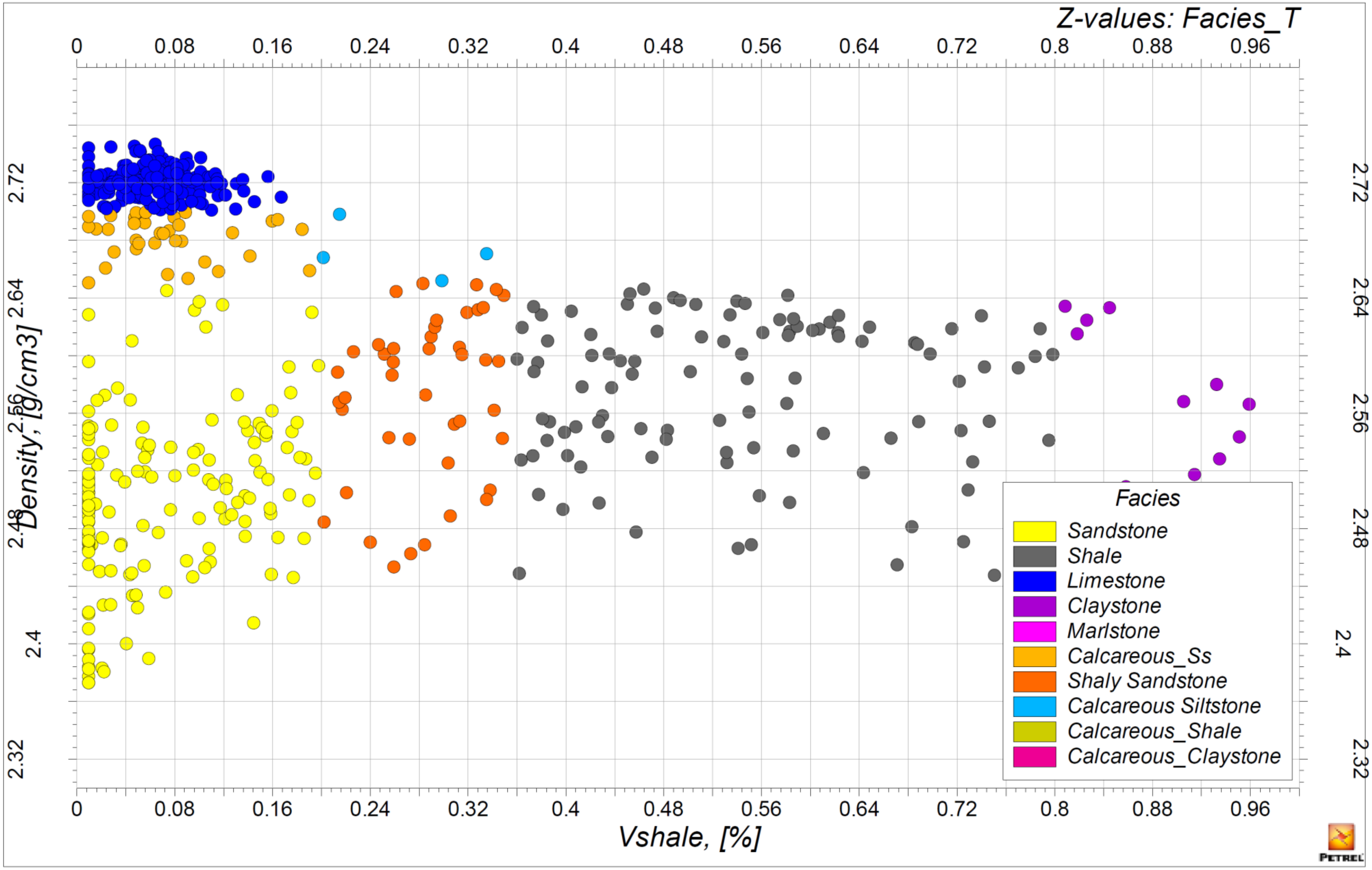

Figure 5. Final crossplot for the facies modelling.

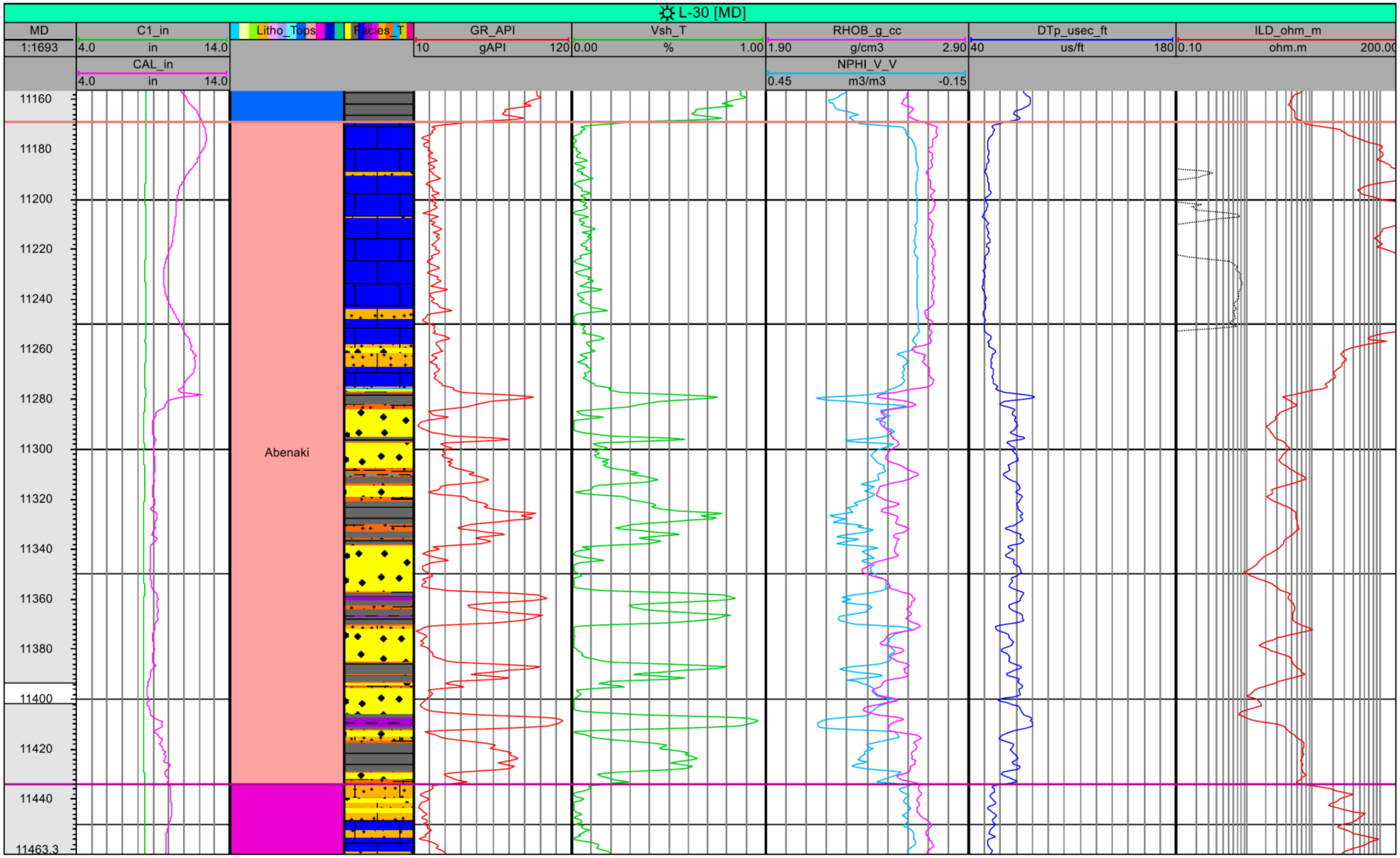

Figure 6. 1D Facies model for the correlation well, obtained applying crossplot interpretation.

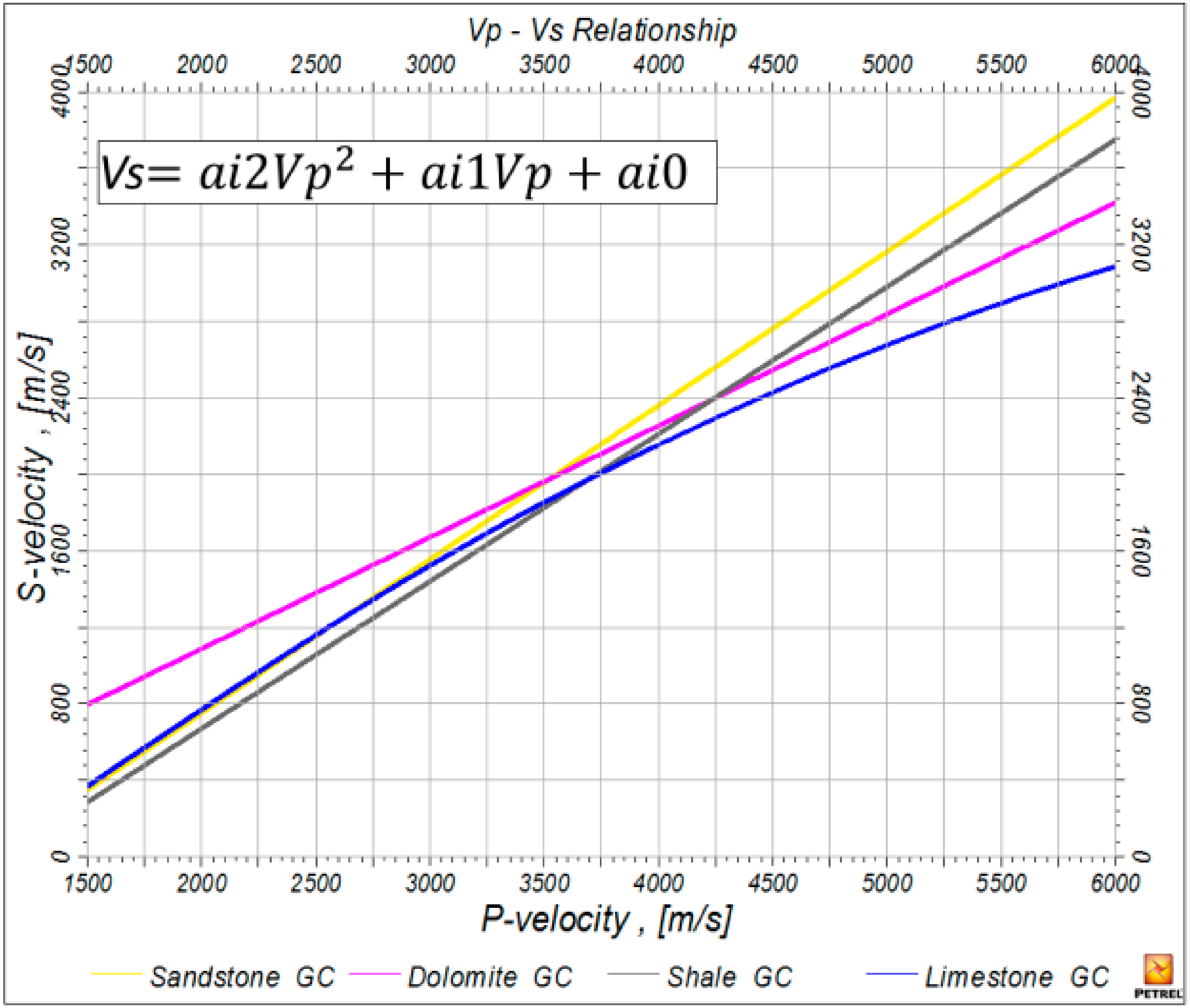

Figure 7. Greenberg- Castagna vs. Vp relationships for different rock types

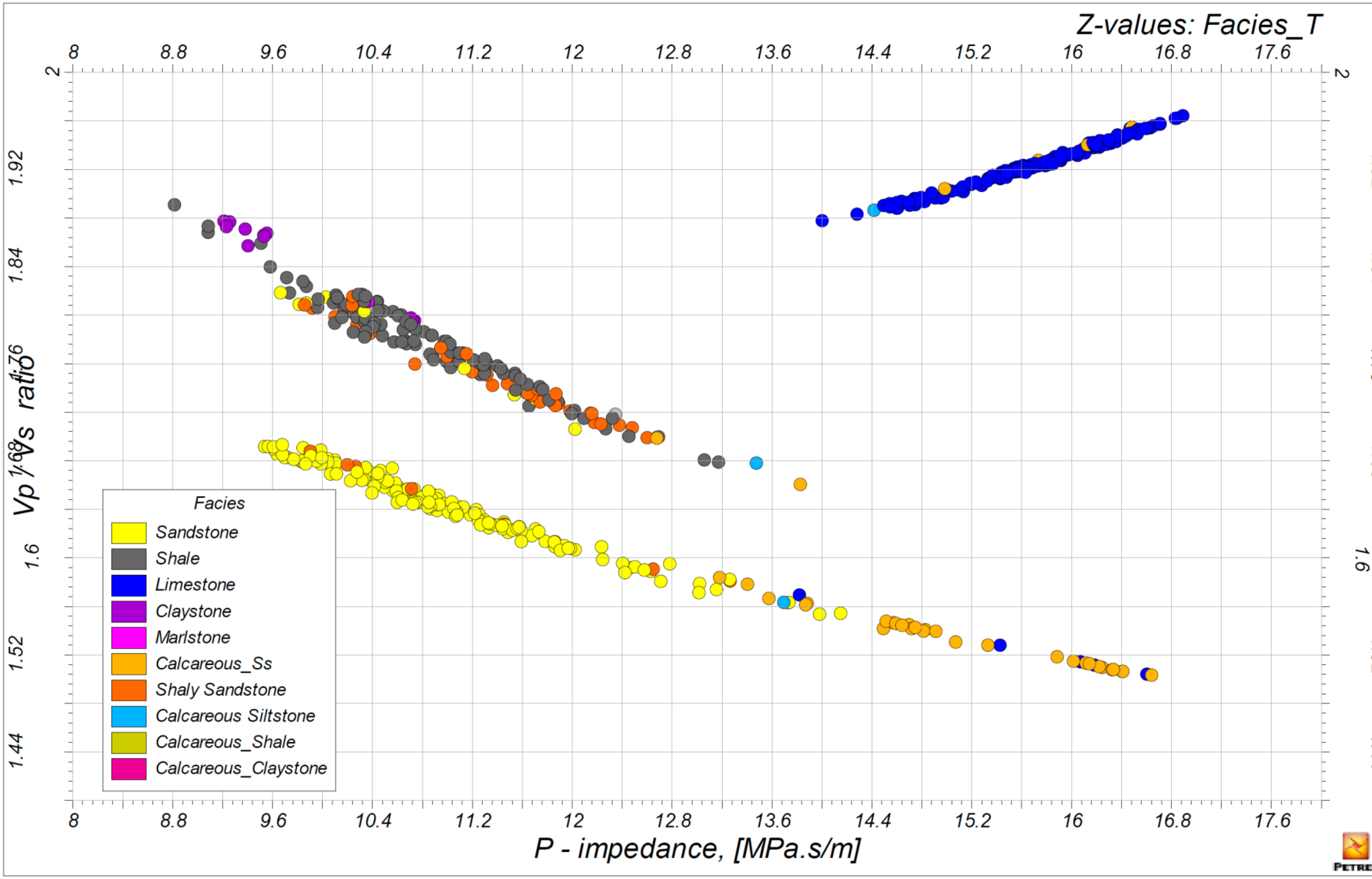

Figure 8. Crossplot of elastic properties, prepared for feasibility analysis of Abenaki Formation.

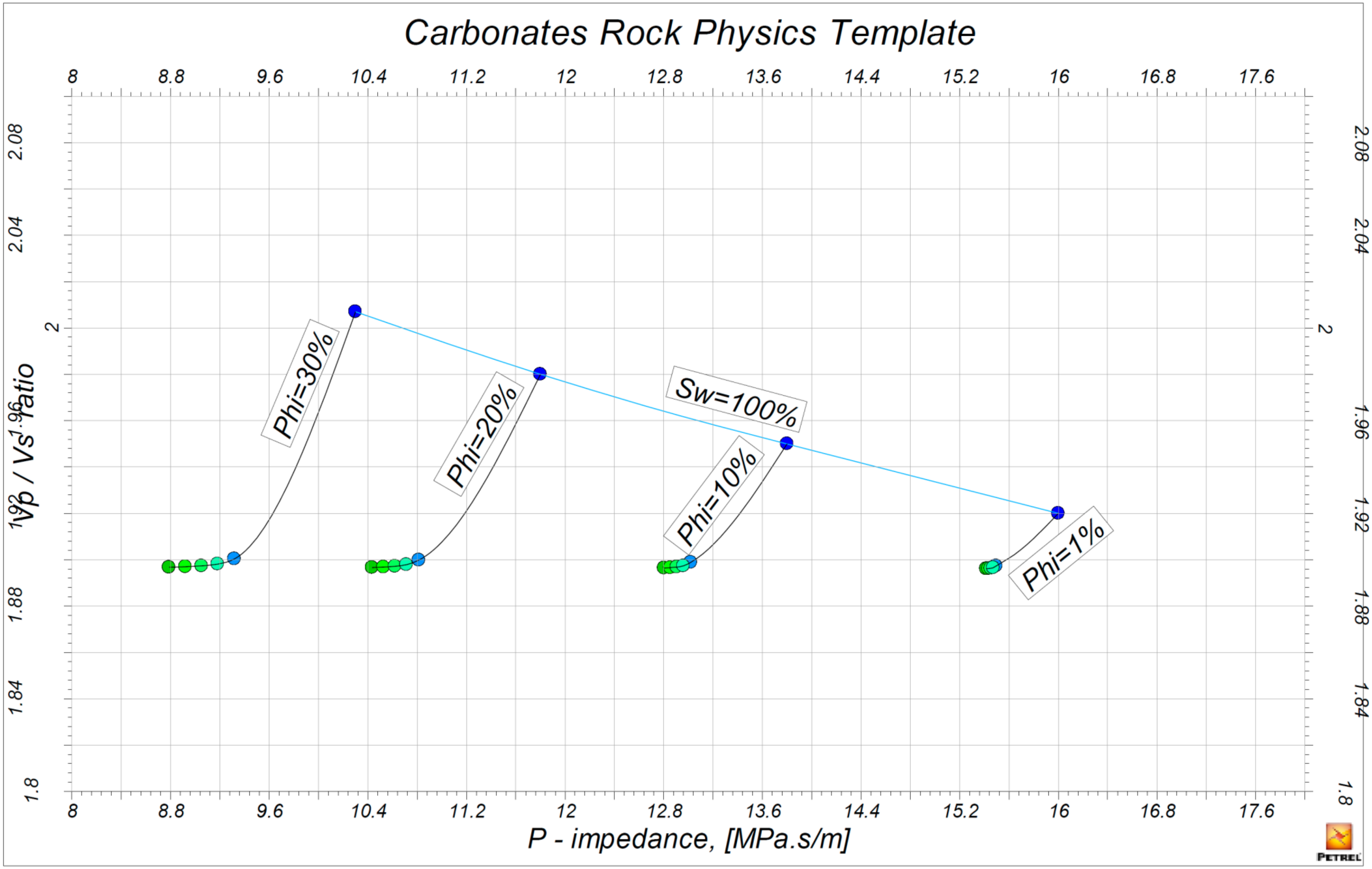

Figure 9. Carbonate rock physics template made for Abenaki Formation.

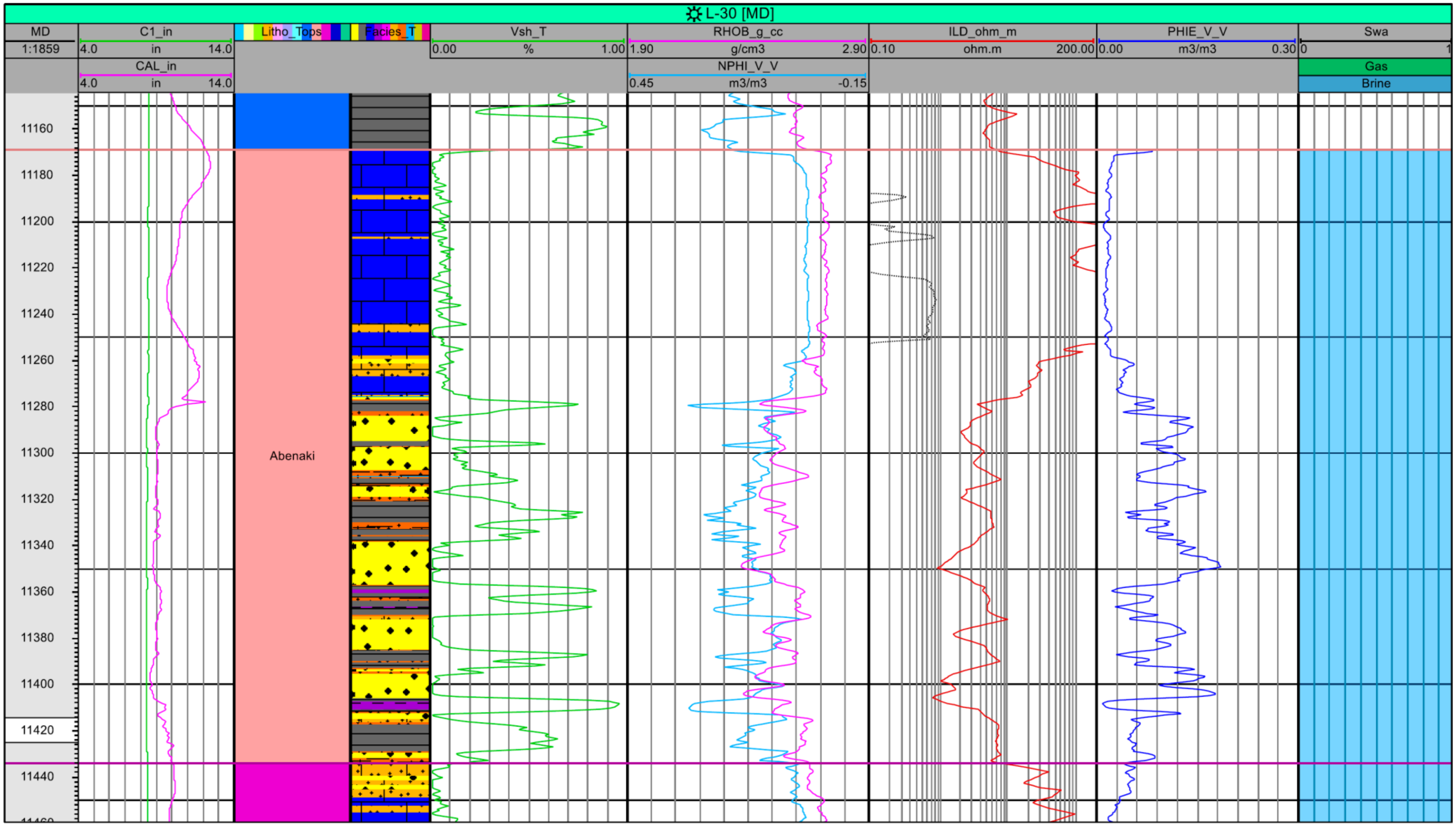

Figure 10. Petrophysical model for the correlation well in Abenaki Formation.

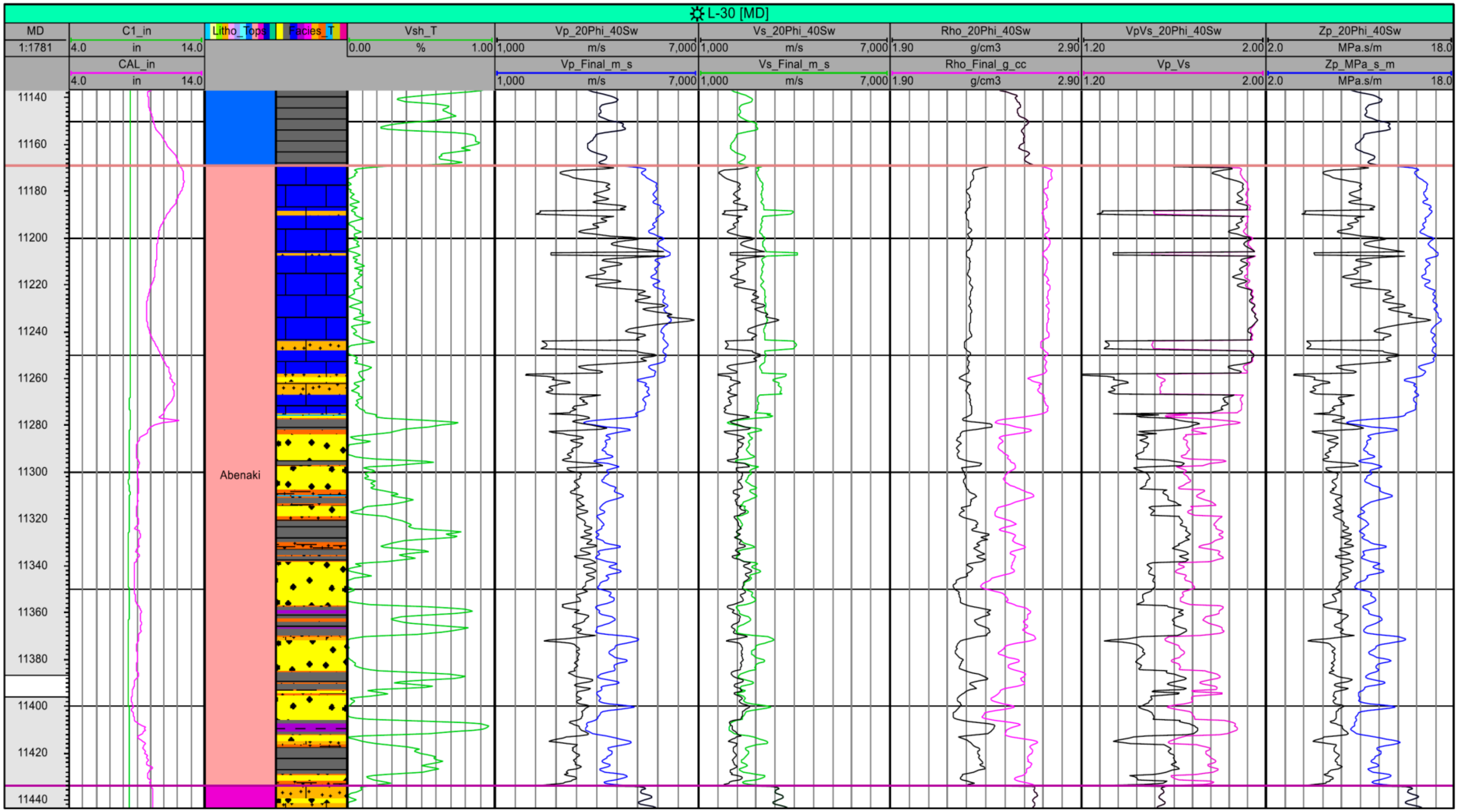

Figure 11. Fluid substitution result for Abenaki Formation. Note the contrast between the change in properties in limestones (blue rock type) for those in sandstones (yellow rock type).

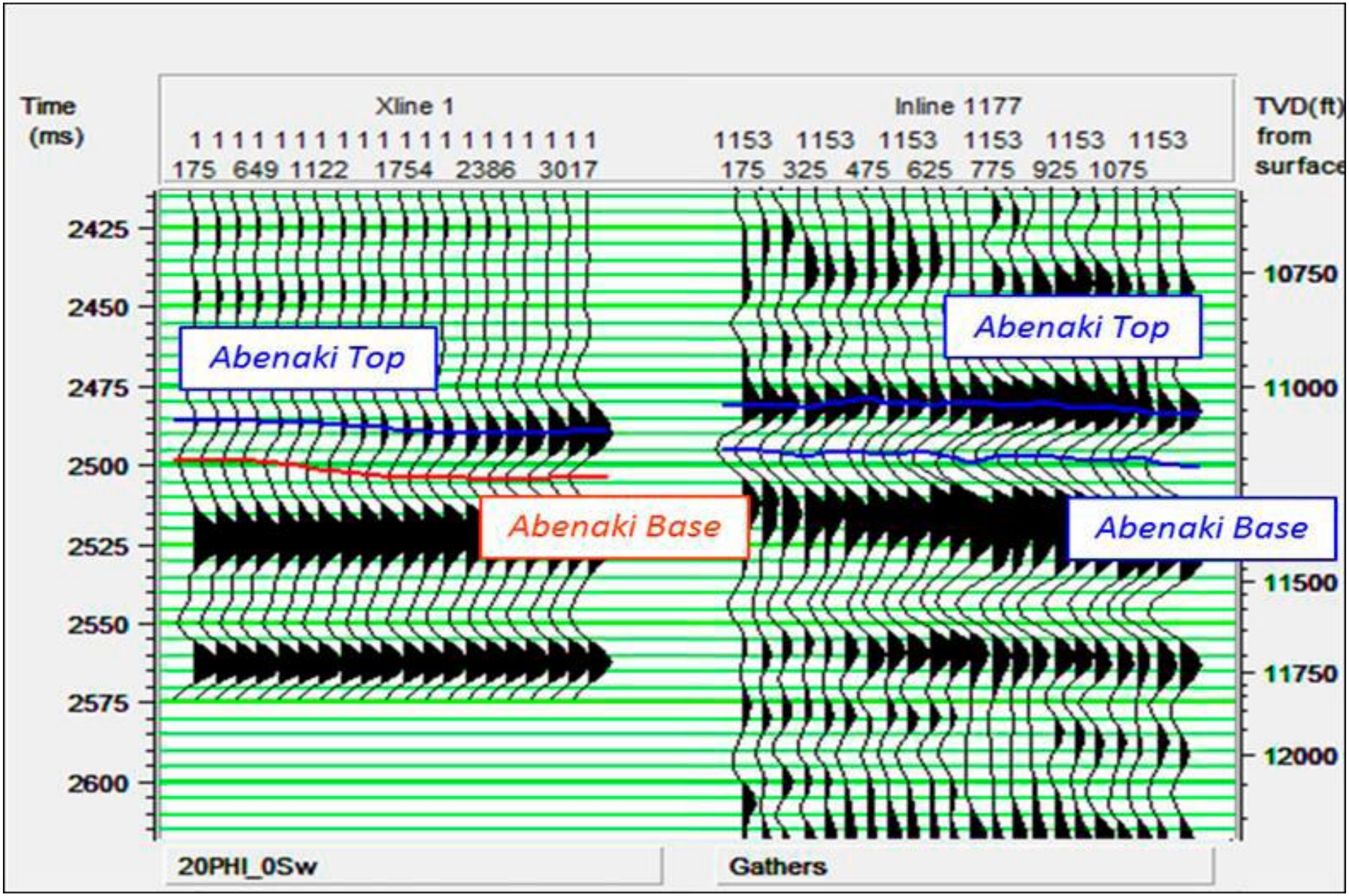

Figure 12. Synthetic gather compared with original gather where both gas saturation and porosity effects on amplitudes can be seen.

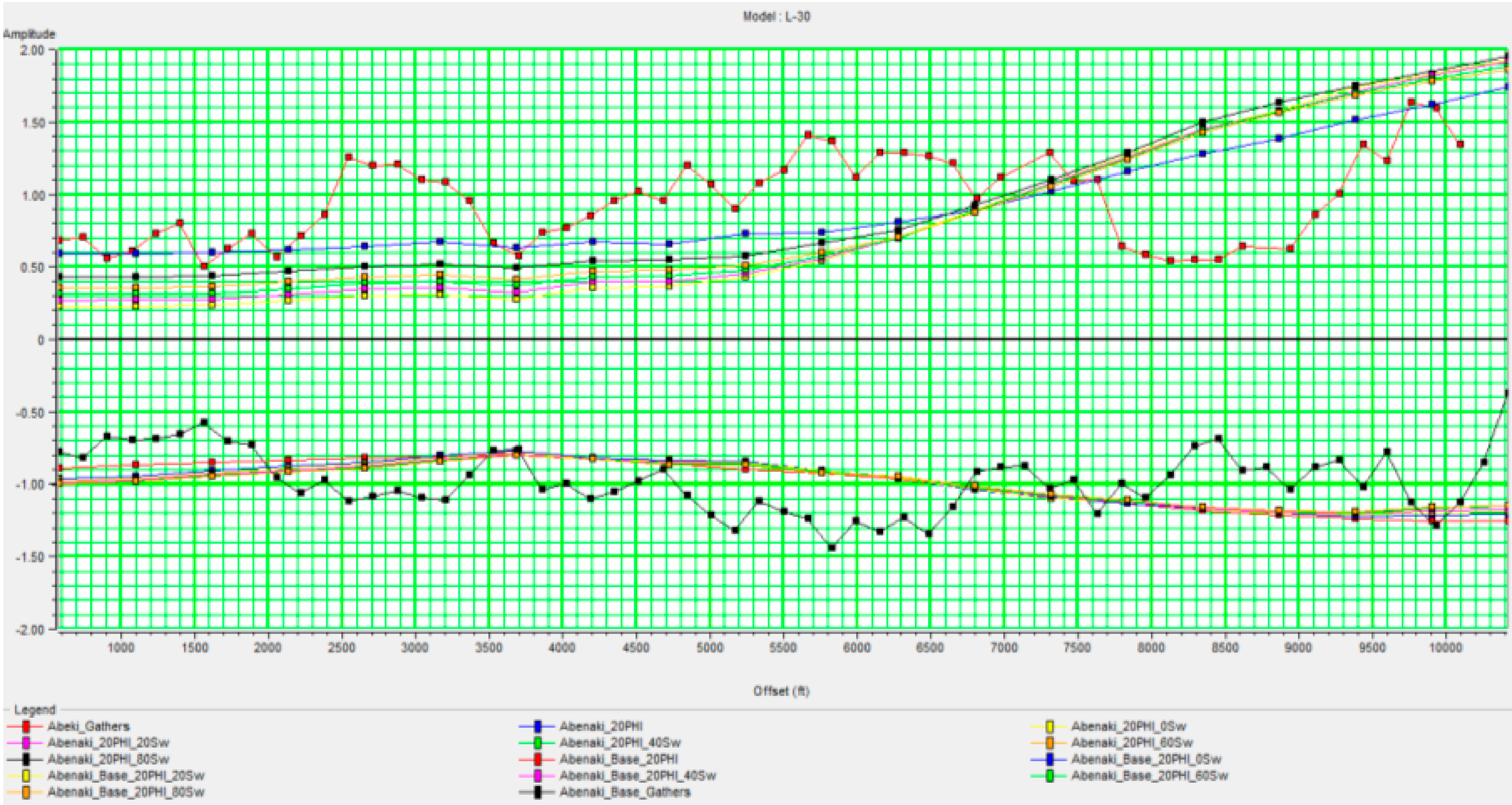

Figure 13. Pickings made for both synthetic and original gathers at the well position.

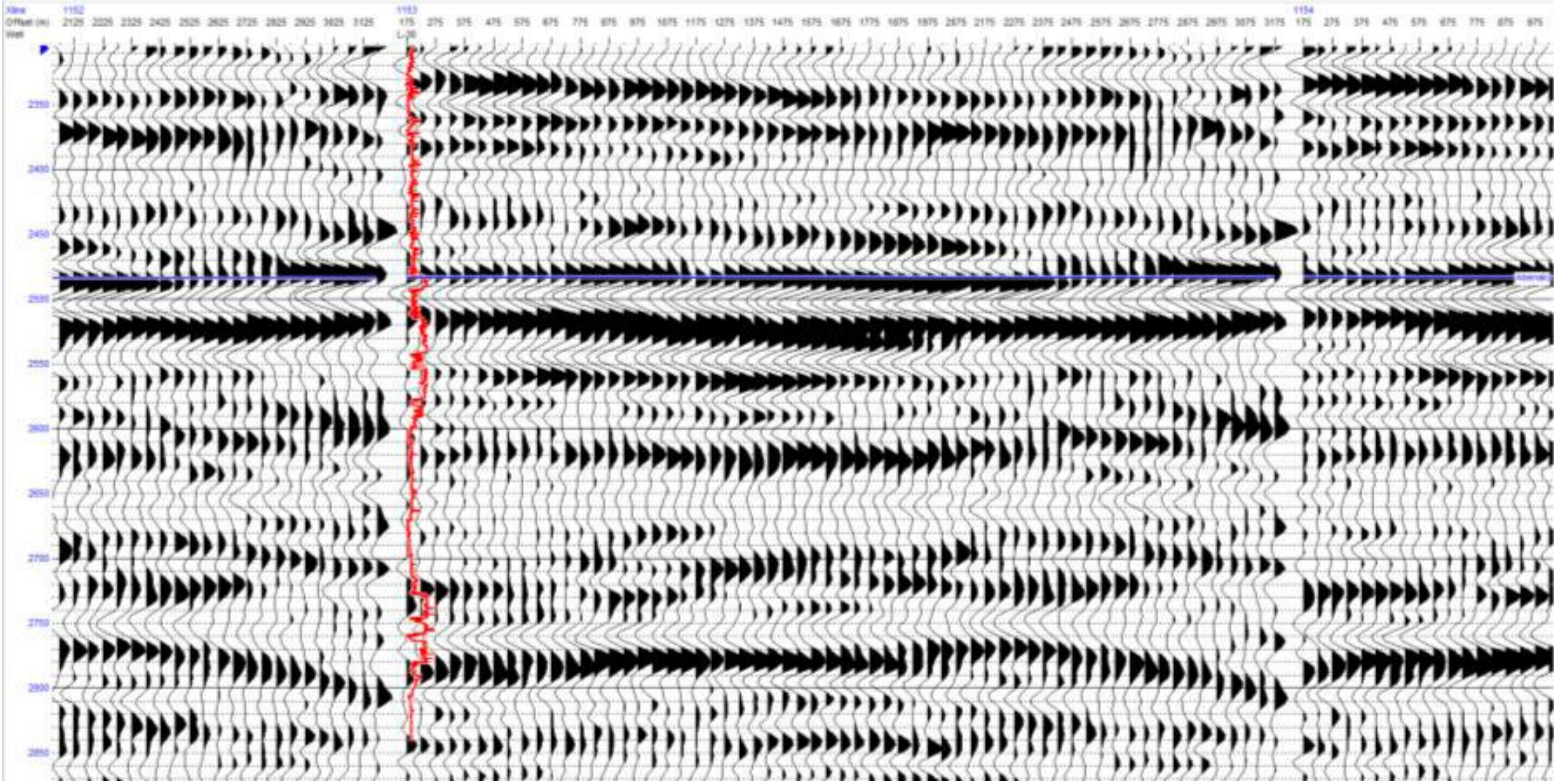

Figure 14. Conditioned seismic gather at the location of the correlation well.

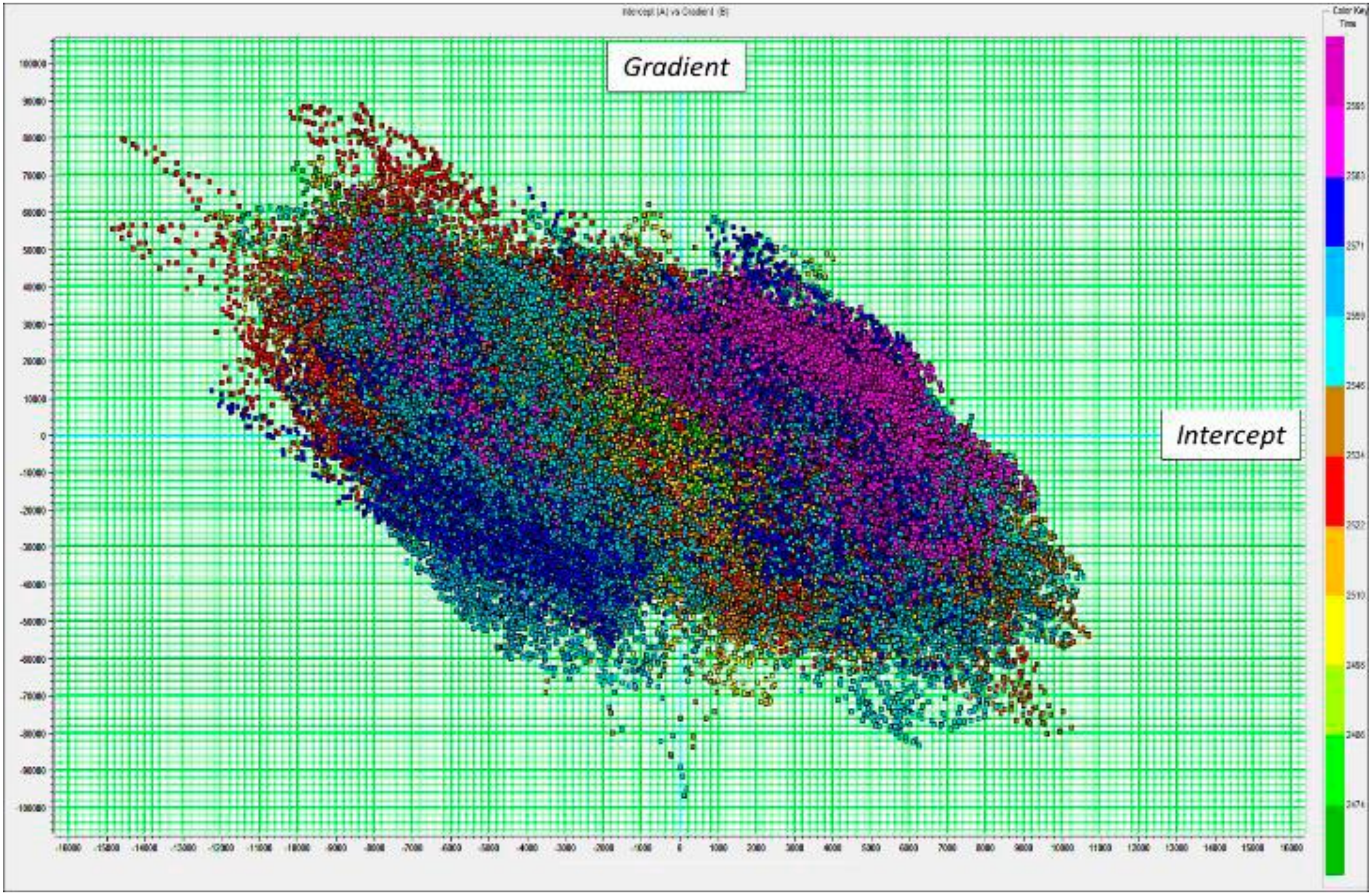

Figure 15. Gradient vs intercept crossplot for Abenaki Formation.

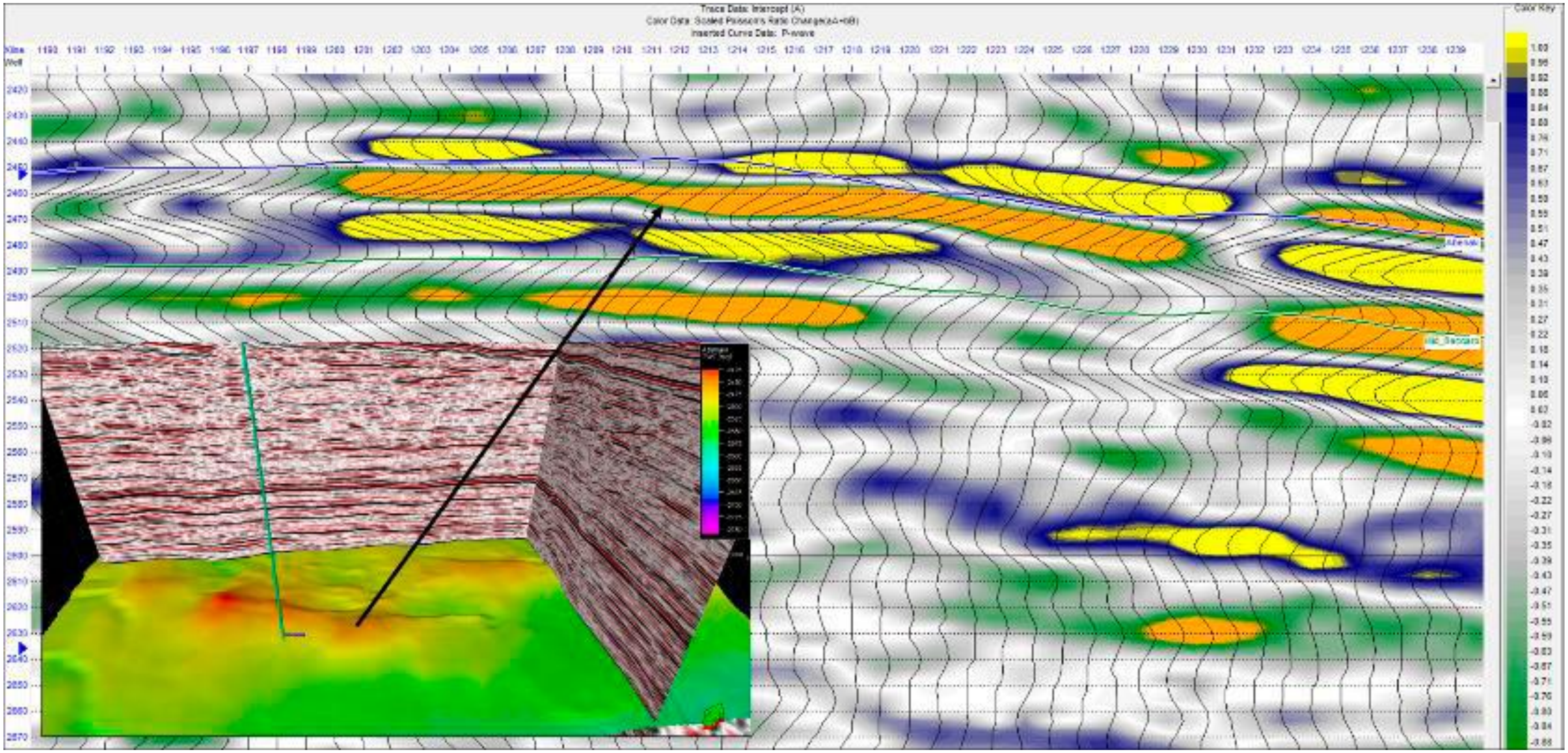

Figure 16. Change of Scaled Poisson's ratio for Inline 1177. A typical AVO Class III anomaly for sandstone was identified at a structural high in Abenaki Formation.

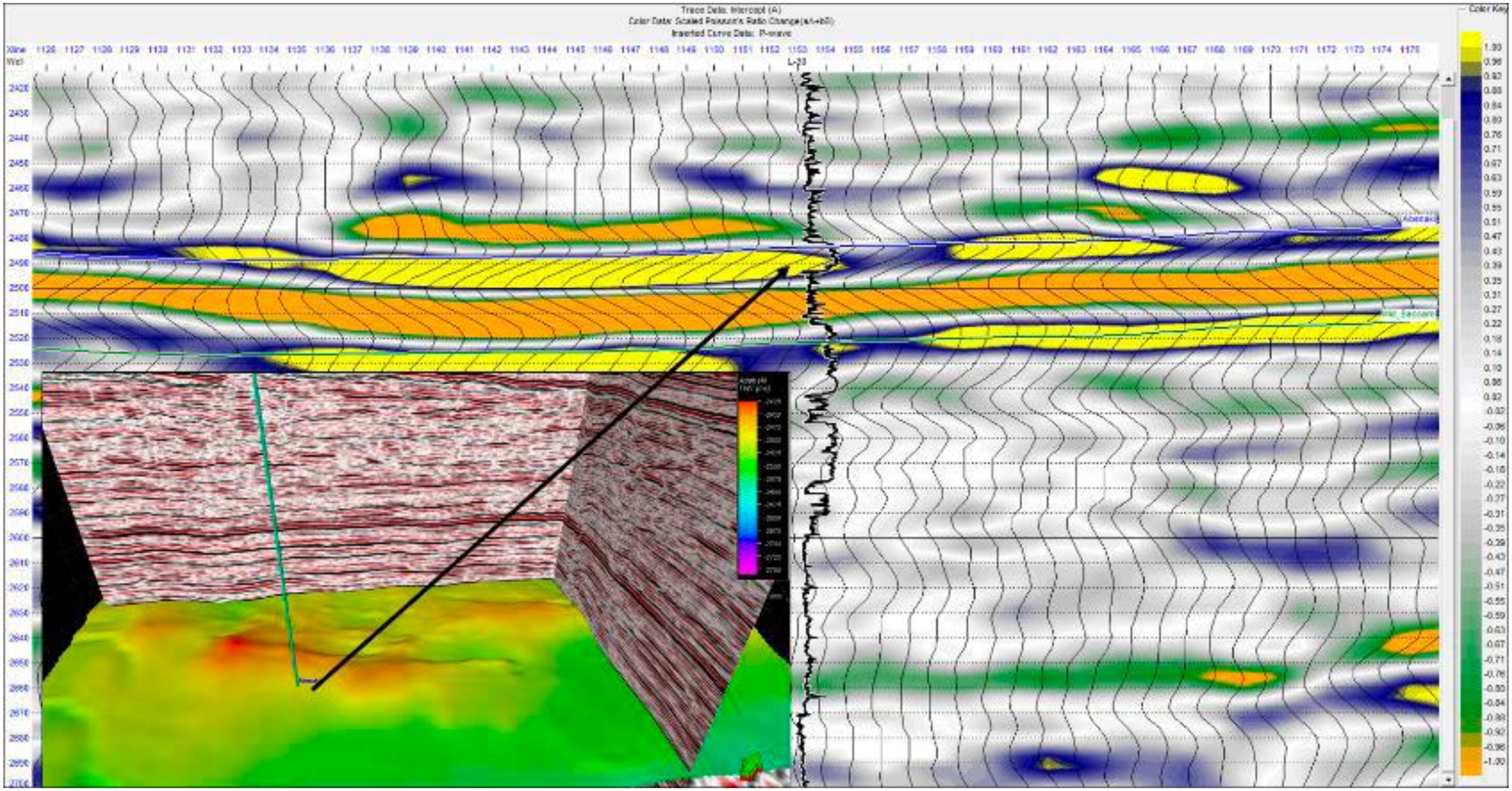

Figure 17. Change of Scaled Poisson's ratio for Inline 1177. Note the response at the L-30 well and nearby areas for the non-porous, dry carbonates, as represented by the yellow color in the Abenaki Formation

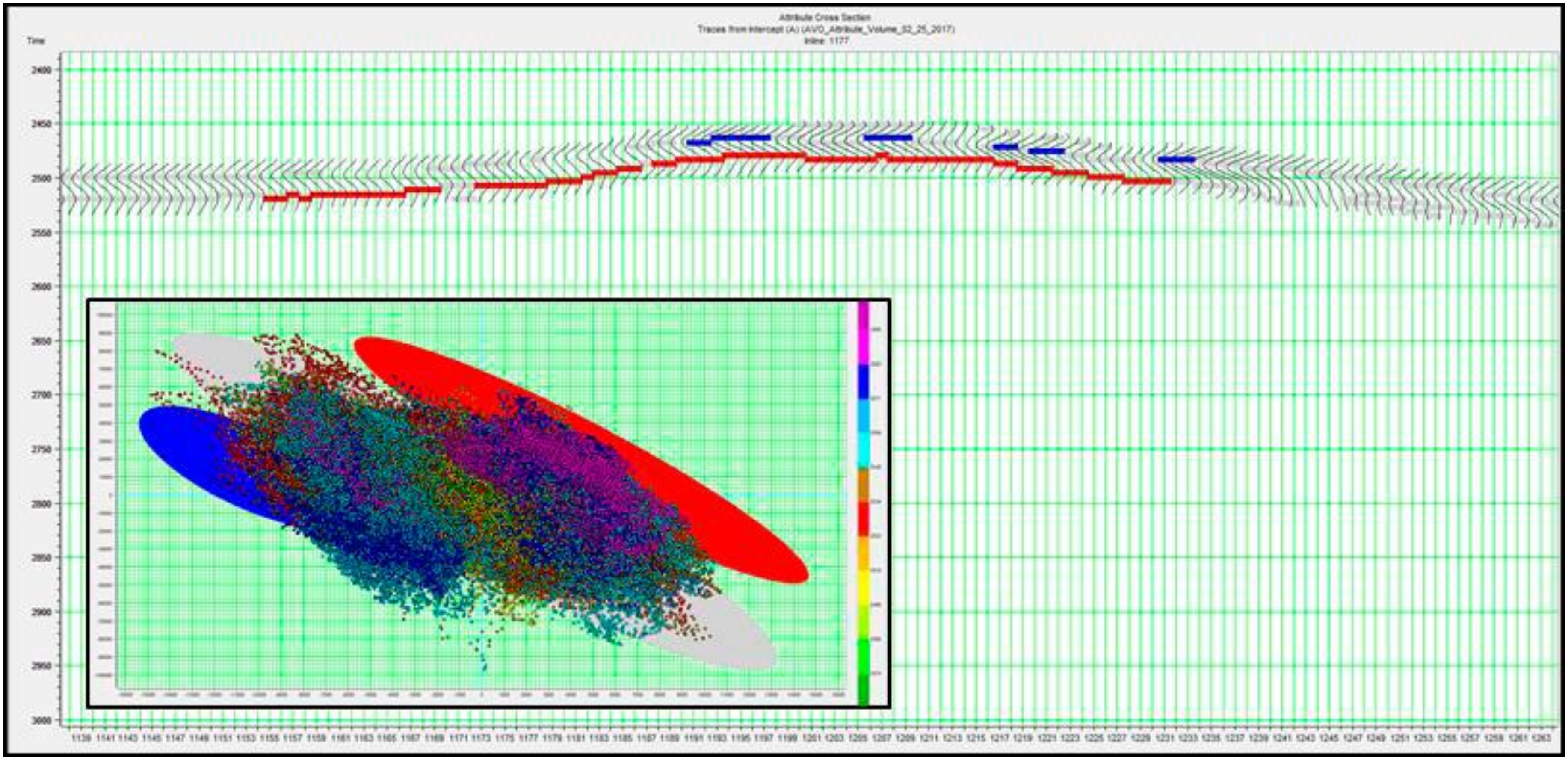

Figure 18. Gradient-Intercept crossplot used to highlight the different carbonate responses. In the section, as in the crossplot, the blue color represents the carbonates of interest, and the red color represents the carbonates with low porosity and high water saturation, as in seen in the well.

Well Log	L-30
Density	x
Neutron Posority	x
Gamma Ray	x
P-Sonic	x
Caliper	x
Deep Resistivity	x
Checkshot	x

Table 1. Well logs available for the correlation well used to characterize the reservoir interval.